OPTIMIZING THE INLINE EMITTERS FOR HIGHER EFFICIENCY SILICON SOLAR CELLS

Abasifreke Ebong, Brian Rounsaville, Ian B. Cooper, Keith Tate, Ajay Upadhyaya and Ajeet Rohatgi,
University Center of Excellence for Photovoltaic Research and Education, School of Electrical and Computer Engineering,
Georgia Institute of Technology, 777 Atlantic Drive, Atlanta, GA 30332-0250

Brian Bunkenburg, Jim Cathey, Steve Kim and Dan Ruf
Despatch Solar, 8860 207th Street West, Lakeville, MN 55044

ABSTRACT: High throughput, low cost and high efficiency are the keys to reducing the cost of photovoltaic electricity. To realize high efficiency, the quality of emitter is critical. The emitter can be formed either by batch deposition of $POCl_3$ gas or inline spray deposition of phosphoric acid (P_2O_5). The $POCl_3$ process has been optimized over the years to give reproducible performance, whereas the inline diffusion has not been systematically optimized. This paper reports on solar cell results achieved with the inline emitters. We have used sheet resistance mapping tool to optimize the emitter uniformity (which is critical to contact formation), junction depth and phosphorus surface concentration to characterize the inline emitters. We have achieved average efficiencies of 17.1% and 17.4%, respectively, on 2 ohm-cm textured CZ with 45 and 60-Ω/sq emitters. Average fill factor of 0.772 and ideality factor of 1.06 suggest the front contact firing was optimized for the inline emitters. PC1D modeling of the 60-Ω/sq emitter showed that efficiency of >18% is achievable by reducing the front surface recombination velocity to 80,000 cm/s and increase the fill factor to 79.5% .

Keywords: spray-on, inline diffusion, ILD, belt-emitter, screen-printed, solar cell, fast firing

1.0 INTRODUCTION

The silicon solar cell performance is controlled by the quality of the p-n junction and its impact on the bulk lifetime during the phosphorus deposition and drive-in. Phosphorus emitters for solar cells can be formed by spray, spin or print deposition of dopant followed by a belt furnace drive-in or by a liquid source using $POCl_3$ gas in a conventional tube furnace. We have shown in our previous work [1] that two-sided phosphorus spin-on, where the back of the wafer is separated from the belt by the phosphorus glass before drive-in can prevent contamination during belt-diffusion. Hoornstra and others [2] reported on the in-line diffusion with the Despatch inline diffusion furnace using spray-on phosphoric acid based dopants. It was also noted that the two sided spray is not only preventing the belt contamination but aids impurity gettering. Voyer and others [3] have characterized various aspect on inline emitters and showed best efficiency of 17.5%. In this work we explored the inline diffused (ILD) emitters using Despatch DCF-3630 atomized spray doping and diffusion furnace system to achieve high efficiency. We characterized and analyzed the cells to understand ILD emitters.

One of the qualities of the ILD emitters is the shallow junction depth. As with all shallow emitters, shunting can occur if the emitter is not uniform or the front silver paste is not compatible. Therefore, the choice of front silver paste is critical to form high quality contact and produce low junction leakage current. In this work we first examined the front silver paste that makes high quality contacts to ILD emitters and then used the paste and firing condition to fabricate the rest of the cells.

2.0 EXPERIMENTAL

The CZ monocrystalline silicon materials were textured at Georgia Tech and sent to Despatch Solar for the inline diffusion in their DCF-3630 diffusion furnace. At Despatch, the wafer surface was made hydrophilic before the wafers were sprayed both top and bottom with a phosphoric acid based dopant using a production scale inline doper. Dopant drying was achieved immediately after spraying using an inline convection dryer at 50°C. The wafers were immediately transferred into an IR belt diffusion furnace for drive-in. The belt speed was held constant while temperature change was used to achieve the sheet resistance targets of 45 and 60-Ω/sq with junction depths of ~ 0.25-0.35 μm and peak concentration of 1-3x10^{20} atom/cm^3.

After the diffusion the wafers were sent back to Georgia Tech where the cells were fabricated, characterized and analyzed. Next, all the emitters were edge isolated followed by phosphorus glass removal and DI water rinse. Then the 60-Ω/sq CZ emitters were divided into two groups as shown in Table I. Group C underwent a further surface clean. Next, a single layer low frequency PECVD SiN antireflection coating was deposited on the front of all the samples at 400°C. We then printed the Al back contact and dried at 200°C followed by the front Ag grid printing and dried at 200°C. Finally, all the cells were co-fired in the IR belt furnace after temperature profiling to ascertain the peak firing temperature.

Table I: Summary of ILD emitter process.

Group Number	Emitter type and process
A (45-Ω/sq - mono)	Despatch (two-side phosphorus spray-on)
B (60-Ω/sq - mono)	Despatch (two-side phosphorus spray-on)
C (60-Ω/sq -mono)	Despatch (two-side phosphorus spray-on – extra clean)

2.1 Investigation of front silver paste for ILD emitters

To avoid shunting any emitter with shallow junction, the front silver paste must not contain aggressive glass frit that will etch the emitter fast and deep to destroy the junction. To this end, we examined four front silver pastes (A-D) to select the one that gives low series and high shunt resistances, acceptable ideality factor and high fill factor. Because the contact co-firing is important to achieving high quality screen-printed contacts we first profile the furnace to determine the peak temperature before firing the test cells. In addition, emitter uniformity is critical to achieving uniform contact resistance on a wafer and from wafer to wafer. So, we used the Sherescan to map the inline emitters as shown in Figures 1a and 1b, for the 45 and 60-Ω/sq emitters on CZ material. Both emitters show standard deviations of only 1.4 Ω/sq, which suggest excellent emitter uniformity.

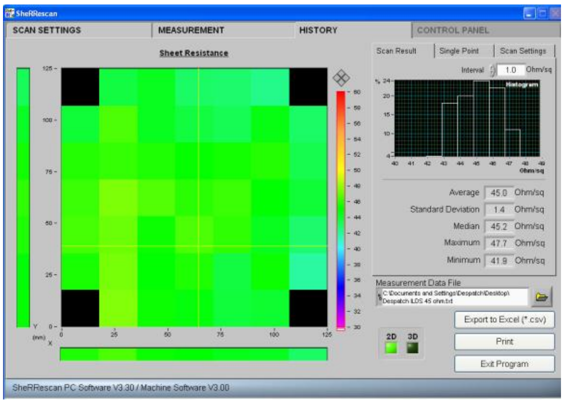

(a)

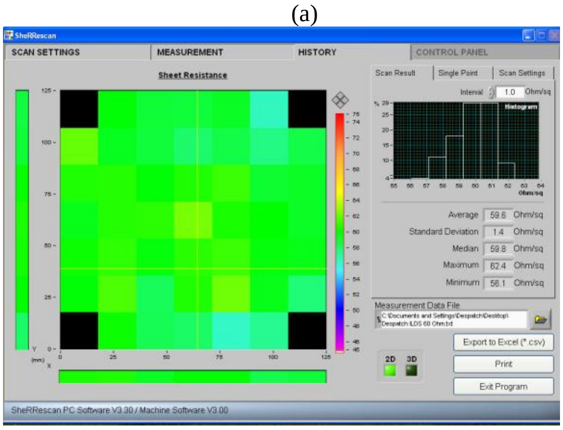

(b)

Figure 1: Sheet resistance mapping for 45 and 60 Ω/sq ILD emitters.

Table II: Summary of front Ag paste selection.

Paste	FF	Rs (Ω-cm^2)	n-factor	Rsh (Ω-cm^2)
A	0.772	0.940	1.06	1949
B	0.759	0.866	1.18	2005
C	0.756	1.001	1.15	3009
D	0.703	2.078	1.2	2915

Table II lists the cell results for the four pastes, with paste A producing the highest fill factor and acceptable ideality factor. Paste B showed lowest series resistance but this advantage was offset by lower fill factor due to high n-factor. However, we did not explore paste B further but chose paste A to make contacts to the ILD emitters.

3.0 RESULTS AND DISCUSSION

3.1 Solar cells with 45-Ω/sq emitters on CZ silicon

Figures 2-4 show the open circuit voltage (V_{oc}), short circuit current density (J_{sc}) and the efficiency (η) distribution for 87 textured monocrystalline CZ 2-Ω-cm with 45-Ω/sq emitters (Group A). Figure 2 shows a mean V_{oc} of 618 mV with standard deviation of 1 mV and a maximum value of 621 mV. Figure 3 shows a mean J_{sc} of 35.8 mA/cm^2 with a standard deviation of 0.166 mA/cm^2 and maximum value of 36.3 mA/cm^2. Figure 4 shows, respectively, the mean and maximum efficiencies of 17.1% and 17.5%. The average efficiency of 17.1% with a standard deviation of only 0.144 is significant and supports the uniformity capability across the ILD emitters as shown in figure 1. The mean fill factor of 0.773±0.005, series resistance of 0.869 ±0.05 Ω-cm^2, ideality factor of 1.05±0.029 and 3000 Ω-cm^2 shunt resistance agrees well with the uniformity across the emitters. Through dark I-V analysis, the leakage current value of 10 nA/cm^2 was obtained. These parameters suggest the front silver paste and the co-firing was suitable to this emitter. However, to achieve higher efficiencies, the V_{oc}, J_{sc} and fill factor must be improved.

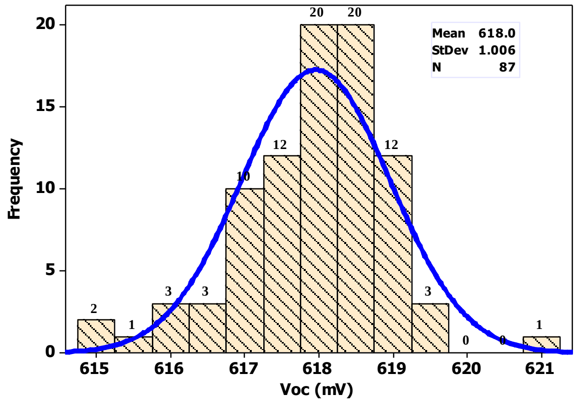

Figure 2: Open circuit voltage distribution for the 45-Ω/sq emitters.

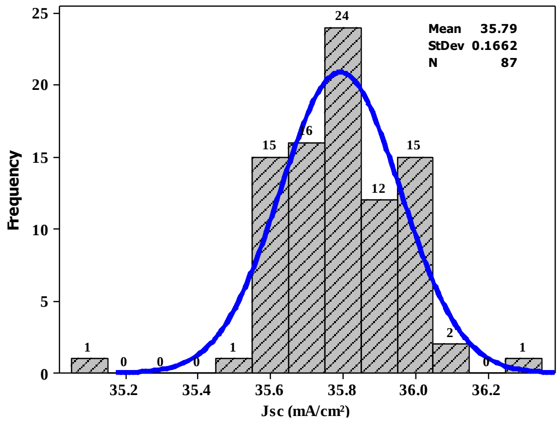

Figure 3: Short circuit current density distribution for the 45-Ω/sq emitters.

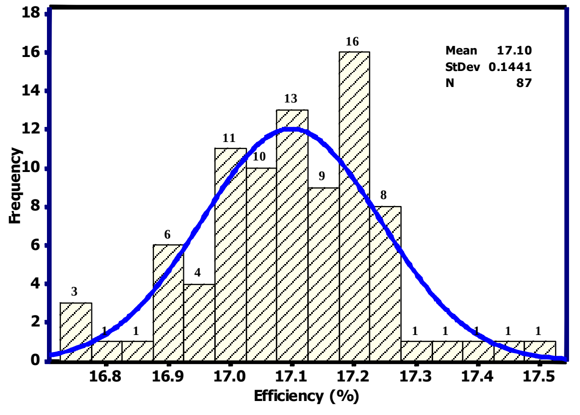

Figure 4: Solar cell efficiency distribution for the 45-Ω/sq emitters.

3.2 Cells with 60-Ω/sq emitters on CZ silicon

Table III: Average electrical parameters for ILD emitters with 60-Ω/sq (Group B and C).

Cell ID	Group B	Group C
V_{oc} (mV)	612	617
J_{sc} (mA/cm^2)	36.1	36.7
FF	0.775	0.769
η (%)	17.1	17.4
n-factor	1.05	1.07
R_s (Ω-cm^2)	0.808	0.883
R_{sh} (Ω-cm^2)	2443	3069

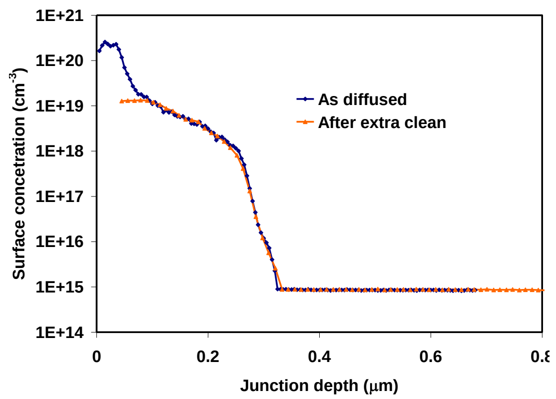

Figure 5: Comparison of as diffused and treated (extra clean) emitter profiles.

Next, we applied the same front silver paste and co-firing conditions to the 60-Ω/sq emitters on mono crystalline CZ wafers. Table III lists the electrical parameters for the two groups of ILD cells with 60-Ω/sq emitters. The mean efficiency for the group B cells is only 17.1% compared with 17.4% for group C. The 0.3% difference is because of the 5 mV in V_{oc} and 0.6 mA/cm^2 in J_{sc}. This gain in V_{oc} (for the group C cells) can be attributed to the increased sheet resistance and a decrease in the surface concentration after the extra clean as suggested by spreading resistance analysis in figure 4. Figure 5 shows two emitters with same sheet resistance; the one which had extra clean shows lower surface concentration than as diffused. Therefore the lower surface concentration led to higher short circuit current density and improved open circuit voltage.

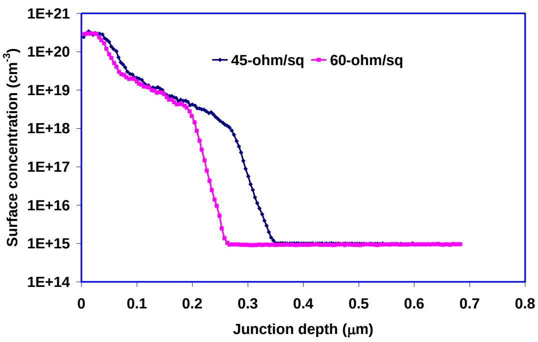

Figure 6: Emitter profiles for the 45 and 60-Ω/sq emitters.

The mean fill factor for group C cells was slightly lower than the group B because of the difference in the series resistance. However, the ideality factor and shunt resistances were not affected. The dark I-V analysis showed the leakage current of 10 nA/cm^2. This result is significant and supports the near perfect uniformity that can be achieved with the inline diffusion. Figure 6 shows the ILD 45 and 60-Ω/sq emitter profiles. Note the surface concentration for the two emitters are similar ~ 2.5x10^{20} cm^{-3}. The junction depths are, respectively, 0.353 μm and 0.267 μm for 45 and 60 Ω/sq emitters. Thus because of the similar front surface concentrations, the group B cells (60-Ω/sq emitters –as diffused) gave the same mean efficiency of 17.1% as the 45 Ω/sq. Note the efficiencies were equal because the V_{oc} advantage of the 45-Ω/sq emitter was balanced by the 0.3 mA/cm^2 advantage in J_{sc} of the group B cells.

3.3 Internal Quantum Efficiency (IQE)

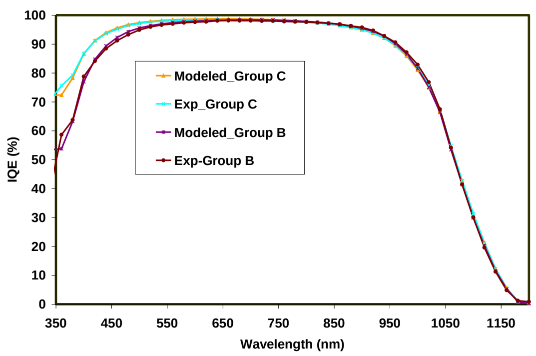

Figure 7: Experimental and modeled IQE for the Groups B and C emitters.

Figure 7 shows the experimental and modeled spectral response for the two groups B and C (60 Ω/sq) emitters. The group C IQE showed higher blue response than the group B emitter. This advantage in blue response with the 5% higher back surface reflectance (PC1D matching of IQE) produced a 0.6 mA/cm^2 difference in J_{sc} between the two groups of cells. The front surface recombination velocity (FSRV) value of 100,000 cm/s and 400,000 cm/s, respectively, fitted the IQE for group

C and B emitters. However, the back surface reflectance (BSR) was different (70% and 65%, respectively for group B and C) for each cell and matched the short circuit currents obtained for each cell. The improved blue response for group C cells is because of the improved carrier collection resulting from the decrease in phosphorus surface concentration as supported by Figure 4.

Table IV: Extracted electrical parameters from IQE measurements and PC1D calculations for the cells.

Cell parameters	Group C-5 17.5%	>18% ILD cell
Base Resistivity (Ω-cm)	2-3	2-3
R_s (Ω-cm^2)	1.1	0.7
R_{sh} (Ω-cm^2)	2877	2877
N_2	2	2
Jo_2 (nA/cm^2)	10	10
Emitter sheet resistance (Ω/sq)	60	60
Surface concentration (cm^{-3})	1.9×10^{20}	1.9×10^{20}
Diffusion length (μm)	384	384
Wafer thickness (μm)	180	180
BSRV (cm/s)	320	320
BSR (%)	70	70
FSRV (cm/s)	100,000	80,000
Grid shading (%)	7.6	7.6
Modeled V_{oc} (mV)	617	618
Modeled J_{sc} (mA/cm^2)	36.7	36.8
Modeled FF (%)	77.2	79.5
Modeled Efficiency (%)	17.5	18.1

Table IV shows the results of modeling and characterization of the group C cells, where the measured and extracted input parameters are listed with the modeled cell efficiencies. Front surface recombination velocity (FSRV) of 1×10^5 cm/s and back surface recombination velocity (BSRV) of 320 cm/s were extracted by matching the measured IQE with the simulated IQE in the short and long wavelength range using PC1D simulation program. The bulk lifetime was measured to be ~50 μs, which corresponds to diffusion length of 384 μm. The junction leakage current of 10 nA/cm^2 was determined by dark I-V analysis and the back surface reflectance (BSR) was found to be 70%. With all the above input parameters, PC1D predicted a cell efficiency of 17.5% with Voc of 617 mV, Jsc of 36.7 mA/cm^2, and FF of 0.772, which agreed well with the measured values. This analysis shows that by improving the FSRV and fill factor greater than 18% efficiency can be achieved with the ILD emitters. The third column in Table IV suggests we need to lower the FSRV to 80,000 cm/s and increase the fill factor to 79.5%. This can be achieved by reducing the front grid coverage, application of high quality dielectric passivation and grid aspect ratio optimization.

4.0 CONCLUSIONS

We have demonstrated the excellent uniformity capability of ILD emitters with both 45 and 60-Ω/sq sheet resistances. We have achieved a mean efficiency of 17.1% and maximum efficiency of 17.5% through a combination of front silver paste, best co-firing and uniform 45 Ω/sq emitters. The mean fill factor of 0.773±0.005, series resistance of 0.869±0.05 Ω-cm^2, ideality factor of 1.06±0.029 and >3000 Ωcm^2 shunt resistance were realized because of the excellent uniformity capability of the ILD emitters.

However, the deeper emitters with the 45 Ω/sq led to average short circuit current density of 35.8 mA/cm^2 which is 0.3 mA/cm^2 lower than the 60 Ω/sq counterparts (Group B) with shallower junction. Although the two emitters have similar surface concentrations, the 60 Ω/sq emitters without the extra clean suffered a loss in V_{oc} and led to the same average efficiency of 17.1%. However, through extra clean of the 60 Ω/sq emitters (Group C), the mean efficiency was increased by 0.3%. This improvement came because of a gain of 5 mV in V_{oc} and of 0.6 mA/cm^2 in J_{sc}. We achieved a mean efficiency value of 17.4% through a combination of front silver paste, best contact co-firing and extra clean of the ILD 60 Ω/sq emitter.

Using the PC1D modeling tool, we were able to match the measured IQE of the group B and C cells. From the matching we extracted the FSRV for group B as 400,000 cm/s and 100,000 cm/s for group C cells. From this modeling, we showed that if the FSRV is reduced to 80,000 cm/s with a fill factor of 79.5 % (through best printing to improve the grid line aspect ratio) the inline emitters will produce efficiencies greater than 18%.

REFERENCES

[1] A. Ebong, V. Yelundur, V. Upadhyaya, B. Rounsaville, A. Upadhyaya, K. Tate, A. Rohatgi and J. Kalejs, "A comprehensive study of the performance of silicon screen-printed solar cells fabricated with belt furnace emitters" Conf. Proc., 20th EPVSEC, Barcelona-Spain, 2005, 1194-1197.

[2] J. Hoornstra, W, van Strueb, M. Lamers, K. Tool and A. Weeber, "High throughput in-line diffusion: Emitter and cell results" Conf. Proc. 22nd EU PVSEC, Milan-Italy, 2007

[3] C. Voyer, D. Biro, K. Wagner, J. Benick and R. Preu, "Fabrication of textured solar cells using sprayed phosphoric acid as the dopant source for the in-line emitter diffusion" Conf. Proc. 21st EUPVSEC, Dresden-Germany, 2006.

ACKNOWLEDGMENTS

The authors will like to thank Mr. V. Upadhyaya, for his many contributions to this work.